Available online at www.sciencedirect.com
SCIENCE DIRECT
Polymer 47 (2006) 5154–5160
polymer
www.elsevier.com/locate/polymer

Vibrational dynamics of *trans*-1,4-polyisoprene (β-form)

Ajita Pathak, Vikal Saxena, Poonam Tandon *, Vishwambhar Dayal Gupta

Physics Department, Lucknow University, University Road, Lucknow 226 007, Uttar Pradesh, India

Received 6 August 2005; received in revised form 16 April 2006; accepted 30 April 2006
Available online 6 June 2006

Abstract

The earlier work on the vibrational dynamics of *trans*-1,4-polyisoprene (β-TPI) suffered from several infirmities. This work has been redone with all infirmities removed. It not only leads to a few different assignments but also better values of interactive constants. Two significant outcomes of the present work are; one change in the profile of the dispersion curves and repulsion between the two acoustic modes at the phase values away from the zone center. The present work leads to a fuller interpretation of observed spectra. Several observed unassigned modes have been accounted for due to the presence of regions of high density-of-states such as von Hove type singularities. Predictive values of heat capacity as a function of temperature are reported.

Keywords: *Trans*-1,4-polyisoprene; Dispersion curves; Density-of-states

1. Introduction

In our earlier publications [1–4] in this journal we have reported several studies on the vibrational dynamics of a variety of polymeric systems including synthetic polymers. In continuation to this work, we report here phonon dispersion in an important industrial polymer namely, *trans*-1,4-polyisoprene (TPI). Polyisoprene is an important polymer widely used in the industry. It finds use in thermoplastic materials used for making telephone hand sets, refrigerator liners safety helmets, radio components, roofing, flooring paints, adhesives. Recently, structural and dynamical behavior of TPI on the local scale has been reported by several workers [5–8].

Raman and infrared (IR) spectroscopic methods have been widely used to study elastomers and polymerized 1,3-dienes in order to determine quantitatively the polymer microstructure. When mono-substituted 1,3-dienes (isoprene) is polymerized, four different structural units may be formed, namely: *cis*-1,4, *trans*-1,4, 1,2-vinyl and 3,4-vinyl. These four possible structures arise from the different polymerization routes. TPI belongs to natural rubber group with general structure $(–CH_2–CH_3{=}CH–CH_2–)_n$. It precipitates from various solvents as single lamellas with crystalline cores and amorphous surfaces or as multilamellar structures depending on crystallization conditions. The nature of the fourfold surface has been investigated by using quantitative chemical reactions in suspension coupled with carbon-13 NMR analysis [9,10].

TPI can exist in two distinct crystalline phases, namely the alpha (α-TPI) and beta (β-TPI) polymorphic forms [11–13]. The α-form has a monoclinic cell with two chains, each containing two repeat units. The β-form has an orthorhombic unit cell with four chains, each containing one repeat unit and *c*-axis fiber repeat distance of 4.70 Å. Crystal structure of β-TPI has been determined by Bunn [14], from X-ray diffraction. Takahashi et al. [15] have also reported the structure of TPI with better resolution for both α- and β-polymorphic forms.

First extensive IR study of synthetic polyisoprene was reported by Binder [16] and several others [17–19] and the assignments from this work were applied to interpret spectroscopic data on natural rubber. Gavish et al. [20] and Mohan et al. [21] have reported a qualitative study of the normal modes of β-TPI using generalized valence force field (GVFF). No dispersion of normal modes is reported. Such studies are reported only by Petcavich et al. [22]. However, they have also used GVFF, which does not take into account non-bonded interactions both in gem and tetra positions and tension terms. Over and above this these authors as well as Gavish et al. [20] have reported only the initial field, which they have transferred from *trans*-1,4-polybutadiene and later refined it. However, none of them have reported the final refined field and this makes a comparison of two fields impossible. This omission hides several features in dispersion profiles and affects the

* Corresponding author. Tel.: +91 522 2782653; fax: +91 522 2740467.
E-mail address: poonam_tandon@hotmail.com (P. Tandon).

0032-3861/$ - see front matter © 2006 Elsevier Ltd. All rights reserved.
doi:10.1016/j.polymer.2006.04.067

absorption bands arising from the regions of the high density-of-states and their contribution to heat capacity via density-of-states. Thus, a fuller interpretation of IR and Raman demands a relook of the vibrational dynamics of β-TPI. Recently, Mohan et al. [21] have reported a qualitative Raman and IR analysis of TPI. However, this paper is a little ambiguous because it is nowhere stated whether the sample which they have studied belongs to the α or the β form or whether it is a mixture of both. It is, therefore, difficult to make any pertinent comment on this work because the spectra reported may be a superposition of both the species. Lack of information on dispersive behavior of normal modes in many polymeric systems has been responsible for incomplete understanding of polymeric spectra.

In the present communication, a detailed comparative study of both polymorphic forms including dispersion curves is presented using Urey Bradley force field. Predictive values of heat capacity in the 10–550 K are presented and a comparative study of the β polymorphic form and α polymorphic form is made to identify the structure-related spectral differences. These are found to be in good agreement with the experimental data. To the best of our knowledge such detailed studies leading to correlation between the microscopic behavior and macroscopic properties have not yet been reported in literature. In general, the IR, Raman spectra and inelastic neutron scattering from polymeric systems are very complex and cannot be unraveled without the full knowledge of dispersion curves. One cannot appreciate without it the origin of both symmetry dependent and symmetry independent spectral features. Further the presence of regions of high density-of-states, which appear in all these techniques and play an important role in thermodynamical behavior, can be studied only from dispersion curves. In this context it may be added that for a fuller justification, one should obtain dispersion curves for a three-dimensional Brillion-Zone with inter-molecular interactions. Thus, the present work is an approximate calculation of the real 3D problem, which is computationally difficult not only because of the dimensionality of the secular matrix but also becomes very large and the interactions increase very rapidly and they are even difficult to visualize.

2. Theory

2.1. Calculation of normal mode frequencies

Normal mode calculation for an isolated polymeric chain was carried out using Wilson's GF matrix [23] method as modified by Higgs [24] for an infinite polymeric chain. The vibrational secular equation to be solved is

$$|G(\delta)F(\delta) - \lambda(\delta)I| = 0 \quad 0 \le \delta \le \pi \tag{1}$$

where δ is the phase difference between the modes of adjacent chemical units, $G(\delta)$ matrix is derived in terms of internal coordinates and inverse of it is kinetic energy and $F(\delta)$ matrix is based on Urey Bradley force field [25] which has certain advantages over other type of force field; such as valence force field, generalized force field.

1. Relatively less parameter are required to express the potential energy.
2. No quadratic cross terms are included in the potential energy expression. The interaction between non-bonded atoms includes these terms.
3. Arbitrariness in choosing the force constant is reduced.

The frequencies ν_i in cm^{-1} are related to eigen values by

$$\lambda_i(\delta) = 4\pi^2 c^2 \nu_i^2(\delta). \tag{2}$$

A plot of $\nu_i(\delta)$ versus δ gives the dispersion curve for the ith mode. The use of the type of force field is generally a matter of one's chemical experience and intuition. In the present work we have used Urey Bradley force field [25] that is more comprehensive then valence force field. Recently, spectroscopically effective molecular mechanics model have been used for inter and intra molecular interactions consisting of charges, atomic dipoles and Vander Waals interactions [26].

2.2. Force constant evaluation

The force constants have been obtained by the least square fitting. In order to obtain the 'best fit' with the observed frequencies, the following procedure is adopted. Initially, approximate force constants are transferred from *trans*-1,4-polybutadiene [27]. Thus, starting with the approximate F matrix F_0 and the observed frequencies λ_{obs} (related through a constant). One can solve the secular matrix equation:

$$GF_0L_0 = L_0\lambda_0 \tag{3}$$

Let $\Delta\lambda i = \lambda i_{obs} - \lambda i_0$ in the above equation. It can be shown that in the first order approximation

$$\Delta\lambda = j\Delta F \tag{4}$$

where j is computed from L_0. We wish to compute the corrections to F_0 so that the errors $\overline{\Delta\lambda}$ are minimized. We use the theory of least square and calculate

$$j'p\overline{\Delta\lambda} = (j'pj)\overline{\Delta F} \tag{5}$$

where p is a weighting matrix and j' is the transpose of j. The solution to this equation is obtained by inverting $j'pj$ to give

$$\overline{\Delta F} = (j'pj)^{-1}j'p\overline{\Delta\lambda} \tag{6}$$

If the number of frequencies is greater than the number of F matrix elements, the matrix $j'pj$ should be non-singular and we obtain the corrections ΔF, which will minimize the sum of the weighted squares of the residuals. If the corrections ΔF are fairly large, the linear relation between force constant and frequency term in the matrix Eq. (a) breaks down. In such a situation, further refinement using higher order terms in Taylor's series expansion of $\Delta\lambda_i$ is needed. This procedure is developed by King et al. [28].

2.3. Calculation of specific heat

Dispersion curves can be used to calculate the specific heat of a polymeric system. For a one-dimensional system the density of state function or the frequency distribution function expresses the way energy is distributed among the various braches of normal modes in the crystal, is calculated from the relation

$$g(\nu) = \Sigma[(\partial\nu_j/\partial\delta)^{-1}]_{\nu_j(\delta)=\nu_j} \quad (7)$$

The sum is over all the branches j. Considering a solid as an assembly of harmonic oscillators, the frequency distribution $g(\nu)$ is equivalent to a partition function. The constant volume heat capacity can be calculated using Debye's relation

$$C_v = \Sigma g(\nu_j) K N_A (h\nu_j/KT)^2 [\exp(h\nu_j/KT)/\{\exp(h\nu_j/KT) - 1\}^2]$$
$$\text{with} \int g(\nu_i)\mathrm{d}\nu_i = 1 \quad (8)$$

3. Results and discussion

The β-form of TPI has planar structure with orthorhombic unit cell with four chains, each containing one repeat unit. The line group of an isolated chain of β-TPI is isomorphs to the point group C_s. The distribution of the normal modes among the irreducible representation for the C_s symmetry is shown below.

C_s	E	σ^{xy}		N_A	O_A
A'	1	1	T_x, T_y, R_z, α_{xx}, α_{yy}, α_{zz}, α_{xy}	25	22
A''	1	−1	T_z, R_x, R_y, α_{yz}, α_{zz}	14	13

T's and α's are dipole and polarizability components. R stands for rotation. N_A, number of normal modes, O_A, optically active modes.

$$T_{vib} = 25A' + 14A''$$

Since, there are four repeat units in the unit cell, we have $4\times6-3=21$ external optical vibrations or 'lattice modes'. Similar calculations can be made for α-TPI. It may be mentioned here that correlation exists between the observed frequencies for the two crystal forms. Each vibrational band in the spectrum for the β-form is correlated to a singlet in a few cases or to a doublet in the majority of cases in the spectrum of the β-form. Such correlation exists even in the amorphous region. It may be added here that we are dealing with an isolated chain, which has a C_s factor group symmetry having only A' and A'' as symmetry species. The site group is necessarily a subgroup of the molecular point group, which describes the symmetry of the free molecule. Hence no additional useful information can be obtained from further symmetry considerations.

The structural repeat unit of β-TPI possesses 13 atoms (Fig. 1), which give rise to 39 dispersion curves. Structural parameters are taken from the work of Gavish et al. [20]. The force constants (Table 1) initially transferred from *trans*-1,4 polybutadiene [27] and modified as given earlier to give the 'best fit' to the observed data [20,21] at the zone center. The frequencies of vibration have been calculated at phase values ranging from 0 to π at intervals of 0.05π. Since, all the modes above 1410 cm^{-1} are non-dispersive in nature, hence the dispersion curves are plotted only for the modes below 1410 cm^{-1}, in Figs. 2(a) and 3(a). The matched frequencies along with their potential energy distribution (PED) are given in Tables 2 and 3. The four modes for which $\omega\rightarrow0$ as $\delta\rightarrow0$ are

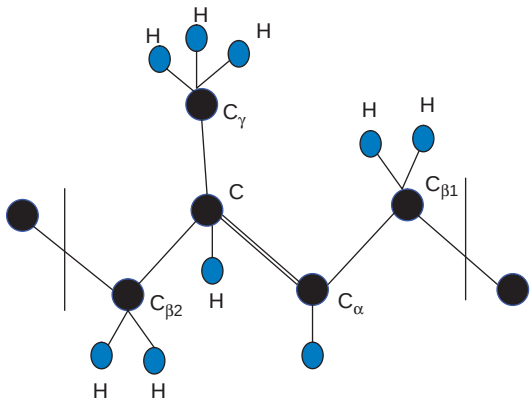

Fig. 1. One chemical repeat unit of β-TPI.

Table 1
Internal co-ordinates and Urey Bradley force constants (mdyn A°)

Internal co-ordinates	Force constants
ν(C=C$_\alpha$)	6.290
ν(C$_\alpha$–H)	4.670
ν(C$_\alpha$–C$_{\beta1}$)	3.190
ν(C$_{\beta1}$–H)	4.070
ν(C$_{\beta1}$–C$_{\beta2}$)	3.480
ν(Cb$_{\beta2}$–H)	4.020
ν(C$_{\beta2}$–C)	2.990
ν(C–C$_\gamma$)	0.520
ν(C$_\gamma$–H)	4.240
ϕ(C=C$_\alpha$–H)	0.349 (0.079)
ϕ(H–C$_\alpha$–C$_{\beta1}$)	0.251 (0.100)
ϕ(C=C$_\alpha$–C$_{\beta1}$)	0.677 (0.450)
ϕ(C$_\alpha$–C$_{\beta1}$–C$_{\beta2}$)	0.790 (0.200)
ϕ(C$_\alpha$–C$_{\beta1}$–H)	0.436 (0.300)
ϕ(H–C$_{\beta1}$–H)	0.322 (0.560)
ϕ(H–C$_{\beta1}$–C$_{\beta2}$)	0.320 (0.320)
ϕ(C$_{\beta1}$–C$_{\beta2}$–H)	0.358 (0.150)
ϕ(H–C$_{\beta2}$–H)	0.310 (0.364)
ϕ(C$_{\beta1}$–C$_{\beta2}$–C)	0.899 (0.350)
ϕ(H–C$_{\beta2}$–C)	0.582 (0.600)
ϕ(C$_{\beta2}$–C–C$_\gamma$)	0.970 (0.339)
ϕ(C$_\gamma$–C=C$_\alpha$)	0.990 (0.400)
ϕ(C$_{\beta2}$–C=C$_\alpha$)	0.839 (0.225)
ϕ(C–C$_\gamma$–H)	0.489 (0.210)
ϕ(H–C$_\gamma$–H)	0.386 (0.200)
ω(H–C)	0.319 (0.290)
ω(C$_\gamma$–C)	0.320
τ(C$_\alpha$–C$_{\beta1}$)	0.009
τ(C$_{\beta1}$–C$_{\beta2}$)	0.013
τ(C–C$_\gamma$)	0.010
τ(C=C$_\alpha$)	0.004

Note: ν, ϕ, ω, τ denote stretch, angle bend, wag and torsion, respectively. Stretching force constants between the non-bonded atoms in each angular triplet (gem configuration) are given in parentheses.

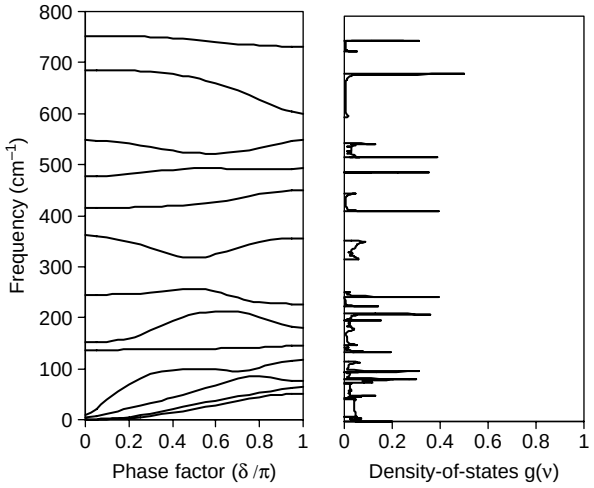

Fig. 2. (a) Dispersion curves of β-TPI. (b) Density-of-states of β-TPI below 800 cm^{-1}.

called acoustic modes. They are due to translations (one parallel and two perpendiculars to the chain axes) and one due to rotation around the chain axis. The agreement between the observed and calculated frequencies is good. The assignments are made on the basis of normal mode calculation, band position, band profile, intensity and appearance/disappearance of similar modes placed in identical environment. For simplicity modes are discussed in two separate sections viz. non-dispersive modes (Table 2) and dispersive modes (Table 3).

3.1. Non-dispersive modes

In general, the non-dispersive modes (Table 2) are the ones that are highly localized in nature. The free stretching modes generally fall in this region; e.g. C–H stretch. CH_2 symmetric and asymmetric stretches appear at (2860, 2841) cm^{-1} and (2924, 2914) cm^{-1}, respectively, and they have little dispersion. Since, the molecule contain two CH_2 groups and

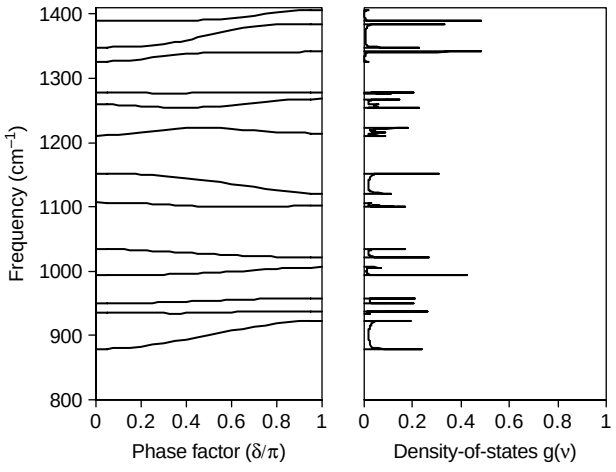

Fig. 3. (a) Dispersion curves of β-TPI. (b) Density-of-states of β-TPI (800–1410 cm^{-1}).

Table 2
Non-dispersive modes of β-TPI

Frequency (cm^{-1})			Assignment (% PED) at $\delta=0$
Calculated	Observed		
	IR[a]	Raman[b]	
3022	3022	3020	ν[C_α–H](100)
2966	2965	2962	ν_{as}[C_γ–H](100)
2924	2943	2930	ν_{as}[$C_{\beta1}$–H](79)+ν[$C_{\beta2}$–H](20)
2914	2914	2912	ν_{as}[$C_{\beta2}$–H](79)+ν[$C_{\beta1}$–H](20)
2896	2906	2880	ν_s[C_γ–H](100)
2894	2906	2880	ν_s[C_γ–H](100)
2860	2855	–	ν_{as}[$C_{\beta1}$–H](100)
2841	2846	2845	ν_{as}[$C_{\beta2}$–H](100)
1666	1664	1666	ν[C=C_α](43)+ϕ[C=C_α–H](16) +ϕ[H– C_α–H](11)
1452	1450	1460	ϕ[$C_{\beta1}$–$C_{\beta2}$–H](29)+ϕ[H–$C_{\beta1}$–H](28)+ ϕ[H– $C_{\beta2}$C](47)
1443	1450	1445	ϕ[H–C_γ–H](92)+ϕ[C–C_γ–H](6)
1434	1430	1432	ϕ[H–$C_{\beta2}$–H](33)+ϕ[H–$C_{\beta2}$–C](27)+ ϕ[H– $C_{\beta1}$–H](17)

[a] Observed frequencies are from Ref. [12].
[b] Observed frequencies are from Ref. [14].

hence the absorption bands appear in pairs. They are slightly displaced from each other because of their placement in different environment and nearness to the CH_3 group. The other pair frequency is given in the parenthesis. The frequencies have been identified with the observed frequencies at (2855, 2846) cm^{-1} and (2943, 2914) cm^{-1}. Similarly, CH_3 symmetric and asymmetric stretches (degenerate) are also non-dispersive and appear close to the observed frequencies as shown in Table 2. It is well established that the deformation vibration $\delta(CH_2)$ gives rise to absorption in the region 1500–1400 cm^{-1}. CH_2 deformation modes are calculated at 1452 and 1436 cm^{-1} that corresponds to the peaks at 1450 and 1430 cm^{-1} in IR spectra. As commented earlier, difference between these modes is due to the different environmental placement of two CH_2 groups.

3.2. Dispersive modes

The modes, which are not localized in nature and are strongly coupled, electrically, mechanically or both show appreciable dispersion, e.g. torsional modes are strongly coupled to the neighboring unit. The actual dispersion of modes is discussed in Section 3.4.

For β-TPI the band at 1348 cm^{-1} was previously assigned by Petcavich et al. [22] to CH_2 wagging and twisting, whereas in the present work it is found to be a mixed mode containing CH_2 twisting and C–C stretching. In fact, CH_2 twisting and CH_2 wagging mode occurs at 1260 cm^{-1} in IR spectra and calculated at the same value in the present work. The rocking mode of CH_2 group gives rise to the medium intensity band at 750 cm^{-1} in infrared and a weak band at 751 cm^{-1} in Raman spectra, as shown in Table 3.

The symmetrical methyl deformation mode $\delta(CH_3)$ is observed at 1384 cm^{-1} in IR and 1386 cm^{-1} in Raman spectra. It is calculated at 1389 cm^{-1}; whereas asymmetric

Table 3
Normal modes and their dispersion in β-PTI

Calculated frequency	Observed frequency		Assignment ($\delta=0$) PED (%)	Calculated frequency	Observed frequency		Assignment ($\delta=\pi$) PED (%)
	IR	Raman			IR	Raman	
1389	1384	1386	ϕ[C–C$_\gamma$–H](49)+ϕ[H–C$_\gamma$–H](42)	1384	1384	1386	ϕ[C–C$_\gamma$–H](53)+ϕ[H–C$_\gamma$–H](45)
1348	1348	1350	ϕ [C$_{\beta1}$–C$_{\beta2}$–H](30)+ν[C$_{\beta1}$–C$_{\beta2}$](22)+ϕ[H–C$_{\beta2}$–H](20)	1341	1348	1350	ϕ [C$_{\beta1}$–C$_{\beta2}$–H](29)+ν[C$_{\beta1}$–C$_{\beta2}$](19)+ϕ[H–C$_{\beta2}$–H](16)
1325	1324	1325	ϕ[H–C$_{\beta2}$–C](32)+ϕ[C=C$_\alpha$–H](18)+ν[C=C$_\alpha$](9)	1329	1324	1325	ϕ[H–C$_{\beta2}$–C](32)+ϕ[C=C$_\alpha$–H](28)
1278	1280	1280	ϕ[C$_\alpha$–C$_{\beta1}$–H](22)+ϕ[H–C$_{\beta1}$–C$_{\beta2}$](21)+ν_{as}[C$_{\beta1}$–C$_{\beta2}$](13)	1277	1280	1280	ϕ[H–C$_{\beta1}$–C$_{\beta2}$](21)+ϕ[C$_\alpha$–C$_{\beta1}$–H](18)+ϕ[H–C$_{\beta1}$–H](15)
1260	1260	–	ϕ[C$_\alpha$–C$_{\beta1}$–H](51)+ϕ[H–C$_{\beta2}$–C](10)	1268	1260	–	ϕ[C$_\alpha$–C$_{\beta1}$–H](25)+ϕ[H–C$_{\beta2}$–C](18)+ϕ[C$_{\beta1}$–C$_{\beta2}$–H](13)
1211	1212	1210	ϕ[H–C$_\alpha$–C$_{\beta1}$](18)+ϕ[C=C$_\alpha$–H](17)+ϕ[H–C$_{\beta2}$–C](16)	1214	1212	1210	ϕ[C$_\alpha$–C$_{\beta1}$–H](42)+ϕ[H–C$_{\beta2}$–C](29)+ϕ[C=C$_\alpha$–H](17)
1152	1150	1151	ν[C$_\alpha$–C$_{\beta1}$](20)+ϕ[C$_\alpha$–C$_{\beta1}$–H](18)+ϕ[C$_{\beta1}$–C$_{\beta2}$–H](10)	1220	1150	1151	ν[C$_{\beta2}$–C](34)+ν[C$_\alpha$–C$_{\beta1}$](14)+ϕ[C$_{\beta1}$–C$_{\beta2}$–C](9)
1107	1107	1109	ν[C$_\alpha$–C$_{\beta1}$](63)+ν[C$_{\beta2}$–C](28)+ϕ[C–C$_\gamma$–H](10)	1102	1107	1109	ν[C$_\alpha$–C$_{\beta1}$](39)+ϕ[C$_\alpha$–C$_{\beta1}$–H](10)
1034	1058	1038	ϕ[C–C$_\gamma$–H](29)+ω[H–C$_\alpha$](12)+ϕ[H–C$_{\beta1}$–C$_{\beta2}$](12)	1021	1058	1038	ϕ[C–C$_\gamma$–H](29)+ν[C$_{\beta1}$–C$_{\beta2}$](19)+ϕ[H–C$_{\beta1}$–C$_{\beta2}$](7)
993	997	1000	ϕ[C–C$_\gamma$–H](39)+ν[C$_{\beta1}$–C$_{\beta2}$](35)	1006	997	1000	ϕ[C–C$_\gamma$–H](39)+ν[C$_{\beta1}$–C$_{\beta2}$](19)+ϕ[H–C$_{\beta1}$–C$_{\beta2}$](11)
950	978	980	ϕ[C–C$_\gamma$–H](39)+ω[H–C$_\alpha$](23)+ϕ [C$_{\beta1}$–C$_{\beta2}$–H](15)	958	978	980	ϕ[C–C$_\gamma$–H](41)+ϕ [C$_{\beta1}$–C$_{\beta2}$–H](13)+ν[C$_{\beta2}$–C](10)
936	962	–	ϕ[C–C$_\gamma$–H](61)+ν[C$_{\beta2}$–C](22)	937	962	–	ϕ[C$_{\beta1}$–C$_{\beta2}$–H](13)+ϕ[C–C$_\gamma$–H](18)+ω[H–C$_\alpha$](18)
879	877	878	ω[H–C$_\alpha$](37)+ϕ[C$_{\beta1}$–C$_{\beta2}$–H](23)+ϕ[H–C$_{\beta2}$–C](14)	923	877	878	ω[H–C$_\alpha$](37)+ϕ[C–C$_\gamma$–H](18)
751	750	751	ϕ[H–C$_{\beta1}$–C$_{\beta2}$](52)+ϕ[C$_{\beta1}$–C$_{\beta2}$–H](13)	730	750	751	ϕ[H–C$_{\beta1}$–C$_{\beta2}$](53)+ϕ[C$_{\beta1}$–C$_{\beta2}$–H](15)
685	600	602	ϕ[C$_{\beta1}$–C$_{\beta2}$–C](20)+ϕ[C–C$_\gamma$=C$_\alpha$](13)+ϕ[H–C$_{\beta1}$–C$_{\beta2}$](10)600	600	600	602	ϕ[C$_{\beta1}$–C$_{\beta2}$–C](20)+ν[C$_\alpha$–C$_{\beta1}$](14)+ϕ[C$_\gamma$–C=C$_\alpha$](13)
476	474	475	ω[C$_\gamma$–C](55)+ϕ[C$_{\beta2}$–C–C$_\gamma$](7)	549	474	475	ω[C$_\gamma$–C](55)+ν[C$_{\beta2}$–C](16)
415	425	–	ν[C–C$_\gamma$](45)+ϕ[C$_\alpha$–C$_{\beta1}$–C$_{\beta2}$](17)+ϕ[C$_{\beta2}$–C–C$_\gamma$](12)	450	425	–	ν[C–C$_\gamma$](41)+ω[C$_\gamma$–C](10)
361	325	380	τ[C=C$_\alpha$](30)+ϕ[C$_{\beta1}$–C$_{\beta2}$–H](14)+ϕ[C$_{\beta2}$–C–C$_\gamma$](12)	355	325	380	ϕ[C$_{\beta2}$–C–C$_\gamma$](28)+ϕ[C$_\alpha$–C$_{\beta1}$–C$_{\beta2}$](24)+τ[C=C$_\alpha$](10)
245	225	–	ϕ[C=C$_{\beta1}$](29)+ϕ[C$_\gamma$–C=C$_\alpha$](24)+τ[C$_{\beta1}$–C$_{\beta2}$](11)	226	225	–	ϕ[C=C$_\alpha$–C$_{\beta1}$](29)+ϕ[C$_\gamma$–C=C$_\alpha$](24)+τ[C$_{\beta2}$–C](11)
151	153	165	τ[C$_{\beta2}$–C](33)+τ[C$_\alpha$–C$_{\beta1}$](20)	146	153	165	τ[C–C$_\gamma$](78)+τ[C=C$_\alpha$](8)
136	130	–	τ[C–C$_\gamma$](90)	117	130	–	τ[C=C$_\alpha$](35)+τ[C–C$_\gamma$](21)

Note: (1) All frequencies are in cm^{-1}. (2) Observed frequencies of IR and Raman are taken from Refs. [12,14], respectively.

methyl deformation mode is assigned to the band at 1450 cm^{-1} in infrared spectra, and it is calculated at 1443 cm^{-1}. The 474 cm^{-1} band calculated at 476 cm^{-1} is predominantly a CH_3 out of plane bending. Bands at 1034, 993 and 950 cm^{-1} are mixed modes containing contributions of the CH_3 and CH_2 rocking and C–C stretching. C–H out of plane bending is responsible for well known band at 870 cm^{-1} in β-TPI. Bands which appear in the region 1100–900 cm^{-1} are associated with C–C skeleton stretch. C–H in plane deformation band is observed at 1212 cm^{-1} in IR spectra and it is calculated at 1210 cm^{-1} as a mode mixed with CH_2 twist.

3.3. Correlation of observed and calculated α- and β-TPI infrared frequencies

A comparison of calculated PED of both the crystal forms shows several differences between them (Table 4). These differences in addition to the environmental factors could arise only from different contents in the unit cell of α-TPI, which contains two residues in a repeat unit and different geometrical parameters. From Table 3 it is obvious that the main difference between the two forms is in the region of CH_3 in plane bending and C–C stretch, which appear at 1348 and 1340 cm^{-1} for β-TPI and α-TPI, respectively. In plane bending (=C–H) was assigned at 1150 cm^{-1} for both forms, by previous workers [22]; which in the present work is separately assigned at 1193 cm^{-1} (α-form) and 1211 cm^{-1} (β-form). These are in good agreement with the observed peaks at 1207 cm^{-1} (α-form) and 1215 cm^{-1} (β-form) in IR spectra. CH_3 and CH_2 symmetric stretching differ by 21 and 36 wave numbers, respectively.

3.4. Characteristic features of dispersion curves

Dispersion curves provide knowledge of the degree of coupling and information concerning the dependence of the

Table 4
Correlation of observed and calculated α- and β-TPI infrared frequencies

Assignments	Frequency (cm^{-1})			
	β Polymorphic form (β-TPI)		α Polymorphic form (α-TPI)	
	Obs. (IR)	Cal. (IR)	Obs. (IR)	Cal. (IR)
CH_3 symmetric stretch	2906	2896	2872	2875
CH_2 asymmetric stretch	2914	2914	2879	2878
CH_3 in plane bending + CH_2 twist (α form)	1348	1348	1340	1340
C–C stretch + CH_3 in plane bending (β-form) CH in plane bending	1212	1211	1205	1193
C–C stretch + CH_3 rocking	997	993	1030	1032
CH_2 rocking	750	751	750	754

Note: Observed frequencies are taken from Ref. [12].

frequency of a given mode upon the sequence length of an ordered conformation. They are also useful in calculating the density of phonon states, which in turn can be used for obtaining thermodynamic properties, such as specific heat, entropy, enthalpy and free energy. It has been observed that the intra molecular interactions (covalent, non-bonded) are generally stronger than the intermolecular interactions (hydrogen bonding and non-bonded). Crystal field only leads to splitting near the zone center and zone boundary. The basic profile of the dispersion curves remains more or less unaltered. Thus, the study of phonon dispersion in polymeric system is an important study. The modes that show large dispersion are either the torsional or rocking mode. Dispersion curves for frequencies below 1410 cm^{-1} are plotted in Figs. 2(a) and 3(a), because the modes above 1410 cm^{-1} are non-dispersive. Mode at 1389 cm^{-1} due to CH_3 symmetric in plane bending disperses to 1407 cm^{-1}. The mode at 1389 cm^{-1} is almost constant till delta is equal to 0.45π. With further increase in δ, this in plane bending mode mixes with (C=C–H) in plane bending and gets coupled. This coupling is responsible for the rising slope of dispersion curve. Band at 1348 cm^{-1} at the zone center, is a mixed mode consisting 30% contribution of CH_2 twisting and 22% contribution of C–C stretching. On moving towards the zone boundary; at $\delta = 0.37\pi$, CH_3 bending mode mixes with ν(C–C) and it rises to 1357 cm^{-1}. In plane (C=C–H) bending appears at 1210 cm^{-1} at the zone center and its contribution progressively falls down with increase in delta value. During its progression it mixes with CH_2 twisting and this energy sharing may be responsible for its reduced dispersion. CH_2 twisting mode at 1152 cm^{-1} at $\delta = 0$; disperses by 68 wave numbers. This downward dispersion may be again due to the sharing of energy with C–C stretching (20–39%) and with CH_2 twisting (18–8%). Peak at 879 cm^{-1} is also due to out of plane bending mode of (C=C–H) with PED $\omega[H–C_\alpha](37) + \phi[C_{\beta1}–C_{\beta2}–H](23) + \phi[H–C_{\beta2}–C](14)$ at the zone center. The other dispersive modes and their PEDs are shown in Table 3. Bands below 400 cm^{-1} are mainly torsional vibrations and they are heavily mixed with in plane bending [(C–C–C), (C–C=C), (C=C–C)]. The PED of (C=C) torsional vibration (361 cm^{-1}) is $\tau[C=C_\alpha](30) + \phi[C_{\beta1}–C_{\beta2}–H](14) + \phi[C_{\beta2}–C–C_\gamma](12)$ at the zone center and it reduces to 355 cm^{-1} at the zone boundary $\phi[C_{\beta2}–C–C_\gamma](28) + \phi[C_\alpha–C_{\beta1}–C_{\beta2}](24) + \tau[C=C_\alpha](10)$. The only other mode, which deserves to be mentioned, is the band at 151 cm^{-1}, which goes through region of high density-of-states at 213 cm^{-1} and, finally dips to 146 cm^{-1}. An interesting feature is displayed by two acoustic modes which repel each other at $\delta = 0.78\pi$. Their frequencies are 96 and 86 cm^{-1}. As expected they exchange PEDs at the point of repulsion. Such exchange of PED and repulsion are indicative of the modes belonging to different symmetry. This is almost like a collision between two quasi particles, which have the same momentum and exchange their energies after collision. The placement of regions of high density-of-states at $\delta = 0.50$ and 0.75 also refer to some internal symmetry points in the energy momentum space and are known as von Hove type singularities. No crossing is present in the dispersive profile of the modes.

3.5. Comparison between dispersion curves

Dispersion profiles of two isolated polymorphic forms without any intermolecular interactions are shown in Fig. 4. A comparison of four acoustic modes in the two forms shows that they have the same general profile, but the peak positions in these differ. The only other difference is the repulsion between the two acoustic modes at $\delta = 0.78\pi$, point at which they repel and exchange their PEDs. Such repulsion is not present in

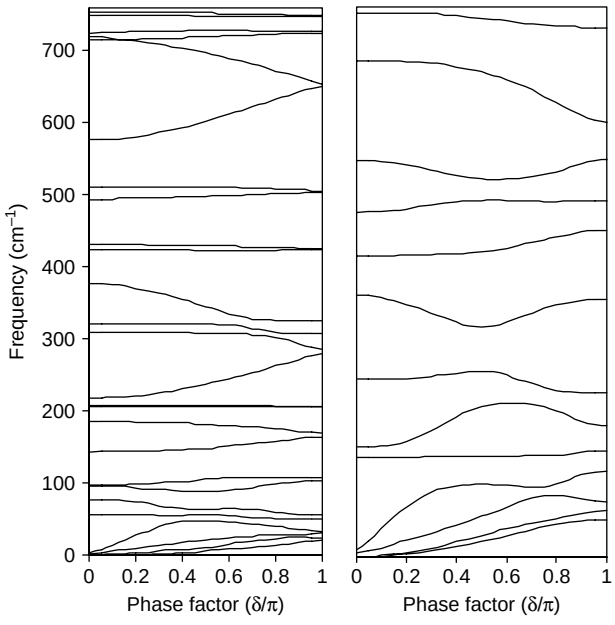

Fig. 4. Comparison of dispersion curves of α- and β-TPI below 760 cm^{-1}.

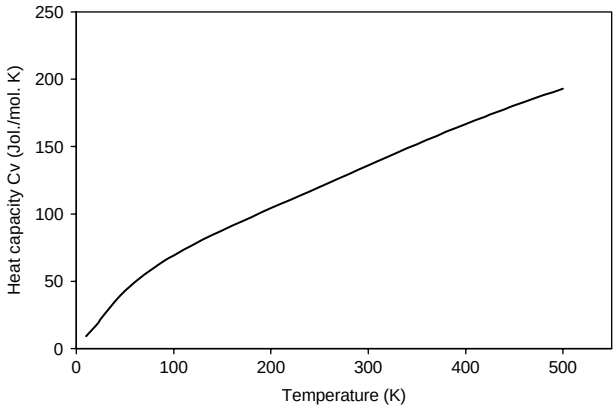

Fig. 5. Variation of heat capacity of β-TPI as a function of temperature.

α-polymeric form. The other major difference is in the dispersion profile of the modes, which appear at 715 and 576 cm^{-1} in the β-polymeric form. This mode converges to 652 cm^{-1} as they progress from the zone center to the zone boundary. The corresponding mode in α polymorphic form is present at 685 $cm^{-1}(\delta=0)$ and 600 $cm^{-1}(\delta=\pi)$. To a smaller extent same features are observed in the two lower dispersion curves of C–CH_3 out of plane bending mode, which converge at 506 cm^{-1}. This mode is of almost non-dispersive behavior for α-TPI and disperses by 73 wave numbers for β-TPI. As emphasized earlier, this difference in dispersion curve is purely because of different geometry and consequently different interactions. One of the major differences in the two forms is the appearance of several regions of high density of states, in β-form but relatively few in α-form. In β-form, they appear at 521, 317, 256, 213, 100 and 85. These bands have not been assigned to any other normal mode and are relatively weak in strength. In the α-form, they are few in number and generally appear below 150 cm^{-1}. Since, no spectral data is available in this region it is difficult to make any specific comment on them.

3.6. Frequency distribution function and heat capacity

The frequency distribution function (density-of-states); which are inverse of the slope of the dispersion curves are shown in Figs. 2(b) and 3(b). The peaks correspond to the regions of high density-of-states. The frequency distribution function shows how the energy is distributed among various branches of the normal modes. This knowledge of density of states is related to thermodynamic properties like heat capacity, enthalpy, etc. of the polymers. Heat capacity of β-TPI has been calculated in the temperature range of 10–500 K. The predictive values of the specific heat are shown in Fig. 5. The specific heat variation is typical of a one-dimensional system, which has an initial large variation but later on it slows down. It may be added that the three-dimensional picture, specially the lattice modes is not considered in this work. The extension of the present calculations in the ultra low temperature region would be meaningful when the calculation is done with the three-dimensional system. This problem is very difficult not only in terms of prohibitive dimensionality but also in terms of potential field. Many interactions would be even difficult to visualize. In spite of several such limitations involved in the vibrational dynamics and concomitant thermodynamic behavior of polymeric systems, the work on an isolated chain is always a useful starting point.

4. Conclusion

The spectral data for the two forms of *trans*-1,4-polyisoprene (α and β polymorphic forms) can be satisfactorily interpreted from the vibration dynamics based on Urey Bradley force field and the profile of dispersion curves. Typical bands characteristic of the two forms are identified. In addition, the predictive values of heat capacity show typical variation for a one-dimensional polymeric system. The characteristic features such as repulsion of dispersion curves are well interpreted.

Acknowledgements

Financial assistance to one of the authors (PT) from the Council of Science and Technology, UP is gratefully acknowledged.

References

[1] Agrawal A, Misra RM, Tandon P, Gupta VD. Polymer 2004;40:1787.
[2] Misra NK, Kapoor D, Tandon P, Gupta VD. Polymer 2000;41:2095.
[3] Misra NK, Kapoor D, Tandon P, Gupta VD. Polymer 1999;40:6395.
[4] Gupta A, Tandon P, Gupta VD, Rastogi S. Polymer 1997;38:2389.
[5] Van Gunsteren WF, Berendsen HJC. Angew Chem Int Ed Engl 1990;29:992.
[6] Laupretre F, Bokobza L, Monnerie L. Polymer 1993;34:468.
[7] Dlubek G, Fretwell HM, Alam A. Phys Status Solidi A 1998;167:R14.
[8] English AD, Ingfield PT, Jones AA, Zhu Y. Polymer 1998;39:309–13.
[9] Schilling FC, Bovy FA, Anandakumaran K, Woodward AE. Macromolecules 1985;16:2688.
[10] Tischler F, Woodward AE. Macromolecules 1986;19:1328.
[11] Stair R, Coblentz W. J Res Natl Bur Stand 1935;15:295.
[12] Hendricks SB, Wildman S, Jones E. Arch Biochem 1945;7:427.
[13] Williams D, Smith D. J Appl Phys 1937;8:497.
[14] Bunn CW. Proc R Soc London, Ser A 1942;180:40.
[15] Takahasi Y, Sato T, Tadocoro H, Tanaka Y. J Polym Sci, Polym Phys 1973;11:233.
[16] Binder JL. J Polym Sci, A-1 1963;37.
[17] Cornell SW, Koenig JL. Macromolecules 1969;2:546.
[18] Bunce SJ, Edwards HGM. Spectrochim Acta 1993;576:775.
[19] Saunders R, Smith D. J Appl Phys 1949;20:953.
[20] Gavish M, Brennam P, Woodward AE. Macromolecules 1998;21:2075.
[21] Arjunan V, Subramanian S, Mohan S. Spectrochim Acta A 2001;57:2547.
[22] Peteavich RJ, Coleman MM. J Polym Sci Phys 1980;18:2097.
[23] Wilson EB, Decius JC, Cross PC. Moleculer vibrations: the theory of infrared and Raman vibration spectra. New York: Dover Publications; 1980.
[24] Higgs PW. Proc R Soc (London) 1953;A220:472.
[25] Urey HC, Bradley HC. Phys Rev 1931;38:1969.
[26] Qian W, Mirikin NG, Krimm S. Chem Phys Lett 1999;315:125.
[27] Rastogi S, Tandon P, Gupta VD. J Macromol Sci Phys 1988;37(5):683.
[28] King WT, Mills IM, Crawford BL. J Chem Phys 1957;27:455.